

## Fully-Coupled Multiscale Poromechanical Simulation Relevant for Underground Gas Storage

Ramesh Kumar, Kishan; Honorio, Herminio T.; Hajibeygi, Hadi

**DOI**

[10.1007/978-3-031-12851-6\\_69](https://doi.org/10.1007/978-3-031-12851-6_69)

**Publication date**

2023

**Document Version**

Final published version

**Published in**

Challenges and Innovations in Geomechanics

**Citation (APA)**

Ramesh Kumar, K., Honorio, H. T., & Hajibeygi, H. (2023). Fully-Coupled Multiscale Poromechanical Simulation Relevant for Underground Gas Storage. In M. Barla, A. Insana, A. Di Donna, & D. Sterpi (Eds.), *Challenges and Innovations in Geomechanics: Proceedings of the 16th International Conference of IACMAG* (Vol. 3, pp. 583-590). (Lecture Notes in Civil Engineering; Vol. 288). Springer. [https://doi.org/10.1007/978-3-031-12851-6\\_69](https://doi.org/10.1007/978-3-031-12851-6_69)

**Important note**

To cite this publication, please use the final published version (if applicable). Please check the document version above.

**Copyright**

Other than for strictly personal use, it is not permitted to download, forward or distribute the text or part of it, without the consent of the author(s) and/or copyright holder(s), unless the work is under an open content license such as Creative Commons.

**Takedown policy**

Please contact us and provide details if you believe this document breaches copyrights. We will remove access to the work immediately and investigate your claim.

***Green Open Access added to TU Delft Institutional Repository***

***'You share, we take care!' - Taverne project***

**<https://www.openaccess.nl/en/you-share-we-take-care>**

Otherwise as indicated in the copyright section: the publisher is the copyright holder of this work and the author uses the Dutch legislation to make this work public.



# Fully-Coupled Multiscale Poromechanical Simulation Relevant for Underground Gas Storage

Kishan Ramesh Kumar<sup>(✉)</sup>, Herminio T. Honorio, and Hadi Hajibeygi

Faculty of Civil Engineering and Geosciences, Delft University of Technology, Stevinweg 1,  
2628 CV Delft, The Netherlands

k.rameshkumar-2@tudelft.nl

**Abstract.** Successful transition to renewable energy supply depends on the development of cost-effective large-scale energy storage technologies. Renewable energy can be converted to (or produced directly in the form of) green gases, such as hydrogen. Subsurface formations offer feasible solutions to store large-scale compressed hydrogen. These reservoirs act as seasonal storage or buffer to guarantee a reliable supply of green energy in the network. The vital ingredients that need to be considered for safe and efficient underground hydrogen storage include reliable estimations of the in-situ state of the stress, especially to avoid failure, induced seismicity and surface subsidence (or uplift). Geological formations are often highly heterogeneous over their large (km) length scales, and entail complex nonlinear rock deformation physics, especially under cyclic loading. We develop a multiscale simulation strategy to address these challenges and allow for efficient, yet accurate, simulation of nonlinear elastoplastic deformation of rocks under cyclic loading. A coarse-scale system is constructed for the given fine-scale detailed nonlinear deformation model. The multiscale method is developed algebraically to allow for convenient uncertainty quantifications and sensitivity analyses.

**Keywords:** Energy storage · Poromechanics · Inelasticity · Algebraic multiscale method

## 1 Introduction

Scaling up the energy storage technologies have been a worldwide focus of research for a long time. More recently, as the world increasingly shifts from fossil fuel-based energy to green fuels, such as hydrogen, the necessity of designing efficient and sustainable energy storage systems has also gained increasing attentions from the scientific community. A well-known technology, already developed for this purpose, is the storage of natural gas in underground geological formations (known as UGS, i.e., Underground Gas Storage). These storage reservoirs, typically located between 1 to 5 km below the surface, act as a buffer to guarantee a reliable supply of green energy (Trakowski 2019; Hashemi et al. 2021). Depleted oil and gas reservoirs, which offer large-scale storage capacities

(TWh), are well characterized, and often include the already-installed facilities that can be repurposed for UGS (Zivar et al. 2021), thus reducing operational costs. The vital ingredients that need to be considered in UGS include accurate and reliable storage capacity estimation and risk assessment, especially to avoid failure due to changes in the in-situ state of stresses (subsidence, induced seismicity, fault reactivation, etc.). Underground formations are often highly heterogeneous over large (km) length scales. They also exhibit inelastic behaviours which are uncertain to a large extent. These structures also entail complex nonlinear deformations under cyclic loadings (Ramesh Kumar and Hajibeygi 2021). Inelasticity can be modelled through several factors, including creep, viscoplastic and thermoplastic physics. In this work, we incorporate it through empirical creep laws, as pointed out by Firme et al. (2019). Notice also that the power law models, such as Carter's model (Carter et al. 1993) and Arrhenius law to account for temperature dependency, are typical for modelling creep behaviour (Ramesh Kumar et al. 2021).

To capture all the geological heterogeneities demand for field scale sizes, algebraic multiscale strategy is developed (Castelleto et al. 2015; Sokolova et al. 2019; Ramesh Kumar and Hajibeygi 2021) to solve the system at coarse scale. More precisely, this work focuses on simulating sandstone reservoirs by accounting the inelastic deformation and solving the coupled poro-elastic system using a hybrid Finite-Element (FE) - Finite-Volume (FV) scheme, at fine scale for mechanics and flow respectively. Built on this hybrid system, an algebraic multiscale strategy is developed which allows for solving the systems at much coarser scales to accommodate heterogeneity in the domain and nonlinear physics.

In what follows, the coupled consolidation model with creep are presented in sections. Section 3 presents the numerical formulation and Sect. 4 discusses the multiscale strategy. The numerical results are shown in Sect. 5, and Sect. 6 closes the presentation.

## 2 Coupled Consolidation Model

The governing equations considered in this work follow Biot's consolidation theory (Biot 1941). Neglecting gravitational effects, the mass conservation equation for a fully saturated and deforming porous medium can be written as

$$\frac{1}{M} \frac{\partial p}{\partial t} - \nabla \cdot \left( \frac{\mathbf{k}}{\mu} \cdot \nabla p \right) + \alpha \frac{\partial \varepsilon_v}{\partial t} = q, \quad (1)$$

where  $M = [c_f \varphi + c_s(\alpha - \varphi)]^{-1}$ , with  $c_f$ ,  $c_s$ ,  $\varphi$  and  $\alpha$  representing the fluid phase compressibility, solid phase compressibility, porosity and the Biot's coefficient, respectively. Additionally,  $\mu$  represents the fluid phase viscosity,  $\mathbf{k}$  is the absolute permeability (which is a 2<sup>nd</sup> order tensor),  $q$  is the source term,  $\varepsilon_v$  is the volumetric strain of the porous rock, and  $p$  is the fluid pressure.

Considering Terzaghi's effective stress principle, the momentum balance equation is

$$\nabla \cdot (\mathbf{C} : \nabla_s \mathbf{u} - \alpha p \mathbf{I}) = \mathbf{f}, \quad (2)$$

where  $\mathbf{C}$  denotes the 4<sup>th</sup> order stiffness tensor,  $\mathbf{I}$  is the identity 2<sup>nd</sup> order tensor,  $\nabla_s$  is the symmetric gradient operator and  $\mathbf{f}$  is the equivalent of the sum of body forces ( $\mathbf{g}$ ) and fictitious forces caused due to inelastic creep strain, i.e.  $\mathbf{f} = \mathbf{g} + \nabla \cdot (\mathbf{C} : \boldsymbol{\epsilon}_{cr})$ .

Creep is the tendency of a material to continuously deform under the application of an external load. Because this is a time-dependent phenomenon, creep is usually represented by a strain rate and it is highly dependent not just on effective stress  $\boldsymbol{\sigma}'$  but also on temperature  $T$ . For simplicity, this work only considers secondary (stationary) creep which is modelled by using Carter (Carter et al. 1993) and Arrhenius laws to account for stress and temperature dependency, respectively. In this case, the creep strain rate can be expressed as

$$\dot{\boldsymbol{\epsilon}}_{cr} = \frac{3}{2} A e^{-\frac{Q}{RT}} \sigma_{VM}^{n-1} \mathbf{s}, \quad (3)$$

where  $A$  and  $n$  are material parameters,  $\sigma_{VM}$  is the Von Mises stress and  $\mathbf{s}$  is the deviatoric stress tensor,  $Q$  and  $R$  are the activation energy and Boltzmann's constant, respectively. Next we will briefly revisit the numerical method used to simulate the coupled flow-mechanics system, with nonlinear creep as explained above.

### 3 Numerical Formulation

In this work, a hybrid FV-FE formulation is adopted for solving the model equations. Particularly, FV is employed for discretizing the mass conservation equation (Eq. 1) on a three-dimensional structured Cartesian corner-point grid, whereas a FE approach is adopted for solving the mechanical problem (Eq. 2). Although both formulations share the same computation grids, pressure and displacements are stored at different positions, as shown in Fig. 1. The displacements, on the other hand, are stored at the element vertices as in standard Galerkin FE formulations. A staggered grid is employed where the displacements are stored in the vertex and the pressure is stored at the cell centre.

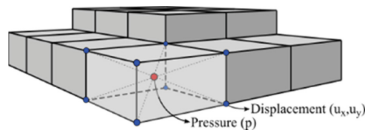


**Fig. 1.** Element of a corner-point grid highlighting pressure and displacement positions.

After discretization with the FV-FE formulation and employing an implicit time integration (i.e., backward Euler), the resulting system of equations can be expressed as

$$\begin{aligned} \mathbf{K}\mathbf{u} + \mathbf{L}\mathbf{p} &= \mathbf{f}^u \\ \mathbf{Q}\mathbf{u} + \mathbf{A}\mathbf{p} &= \mathbf{f}^p \end{aligned} \quad (4)$$

where matrices  $\mathbf{K}$ ,  $\mathbf{L}$ ,  $\mathbf{Q}$  and  $\mathbf{A}$  represent the effective stresses, pressure gradients, volumetric strains and the accumulation terms plus Darcy velocities, respectively. Furthermore,  $\mathbf{f}^p$  contains pressures and volumetric strains from the previous time step, and  $\mathbf{f}^u$  comprises the boundary conditions and the fictitious creep forces.

According to Eq. (3), the creep forces also depend on  $\mathbf{u}$ , since  $\sigma_{VM} = \sigma_{VM}(\mathbf{u})$  and  $\mathbf{s} = \mathbf{s}(\mathbf{u})$ , thus Eq. (4) represents a nonlinear system of equations. For a given time level, the residuals of Eq. (4) for an iteration  $k$  can be expressed as

$$\begin{aligned} \mathbf{r}^{p,k} &= \mathbf{f}^{p,k} - \mathbf{A}\mathbf{p}^k - \mathbf{Q}\mathbf{u}^k \\ \mathbf{r}^{u,k} &= \mathbf{f}^{u,k} - \mathbf{L}\mathbf{p}^k - \mathbf{K}\mathbf{u}^k. \end{aligned} \tag{5}$$

Following Newton’s method, Eq. (5) is expanded by Taylor series, i.e.,

$$\begin{aligned} \mathbf{r}^{p,k+1} &\approx \mathbf{r}^{p,k} + \left. \frac{\partial \mathbf{r}^p}{\partial \mathbf{u}} \right|^k \delta \mathbf{u}^{k+1} + \left. \frac{\partial \mathbf{r}^p}{\partial \mathbf{p}} \right|^k \delta \mathbf{p}^{k+1} \\ \mathbf{r}^{u,k+1} &\approx \mathbf{r}^{u,k} + \left. \frac{\partial \mathbf{r}^u}{\partial \mathbf{u}} \right|^k \delta \mathbf{u}^{k+1} + \left. \frac{\partial \mathbf{r}^u}{\partial \mathbf{p}} \right|^k \delta \mathbf{p}^{k+1}, \end{aligned} \tag{6}$$

and the residuals at the current iteration  $k + 1$  are made equal to zero, which results in the following system of equations

$$\begin{bmatrix} \partial_{\mathbf{u}} \mathbf{r}^u & \partial_{\mathbf{p}} \mathbf{r}^u \\ \partial_{\mathbf{u}} \mathbf{r}^p & \partial_{\mathbf{p}} \mathbf{r}^p \end{bmatrix}^k \begin{bmatrix} \delta \mathbf{u} \\ \delta \mathbf{p} \end{bmatrix}^{k+1} = - \begin{bmatrix} \mathbf{r}^u \\ \mathbf{r}^p \end{bmatrix}^k. \tag{7}$$

Finally, the linearized system of Eq. (7) is iteratively solved monolithically for each time step. Within each Newton’s iteration loop, pressure and displacements are updated as  $\mathbf{u}^{k+1} = \mathbf{u}^k + \delta \mathbf{u}^{k+1}$  and  $\mathbf{p}^{k+1} = \mathbf{p}^k + \delta \mathbf{p}^{k+1}$ .

### 4 Multiscale Formulation

Physical phenomena related to underground activities usually involve different scales, with highly heterogeneous material properties. From the numerical perspective, this represents a significant challenge, since the poromechanics system is mathematically global (i.e., parabolic), and thus simulation domain must be as big as the physical geo-system. Any localization, with assumed boundary conditions, will add to the uncertainty of the assessments. Solving on the coarse scale, on the other hand, raises the question of how to properly upscale the physical properties. Classically, homogenization or upscaling approaches have been used to reduce the complexity of the system. However, for geo-systems with heterogeneous coefficients which do not have separation of scales, upscaling leads to significant and uncontrollable error norms.

To address this challenge, a multiscale finite element/finite volume formulation (MsFEM/FVM) in which a coarse-scale grid is superimposed to a finescale grid is adopted (Castelletto et al. 2017). The fundamental concept behind this work is to build the system of equations in the finescale grid and then project and solve it onto the coarse-scale grid. Let us denote the finescale system of equations (Eq. 6) as

$$\mathbf{A}_f \mathbf{x}_f = \mathbf{b}_f, \tag{8}$$

where the subindex  $f$  denotes the finescale grid. Let us denote the number of nodes in the fine and coarse grids as  $n_f$  and  $n_c$ , respectively. For three-dimensional poromechanics,

the dimensions of  $A_f$  and  $\mathbf{b}_f$  are respectively  $(4n_f \times 4n_f)$  and  $(4n_f \times 1)$ . Because, there exists 3 displacements (in each physical dimension) and the scalar pore pressure.

The prolongation (P) and restriction (R) operators are then defined such that the coarse matrix of coefficients and coarse independent vector can be obtained by

$$A_c = R A_f P \quad \text{and} \quad \mathbf{b}_c = R \mathbf{b}_f, \quad (9)$$

respectively. This implies that R and P have dimensions  $(4n_c \times 4n_f)$  and  $(4n_f \times 4n_c)$ , respectively. In this manner, the system of equations to be actually solved is  $A_c \mathbf{x}_c = \mathbf{b}_c$ , which is much smaller than Eq. (7) depending on the chosen coarsening ratio. After solving the coarse-scale system, the fine scale solution can be retrieved through the prolongation operator, that is,  $\mathbf{x}_f = P \mathbf{x}_c$ .

The important detail in the above strategy is how to build matrices P and R, especially when coarsening ratios are big enough to cause high variations of coefficients within each coarse block. These matrices are composed of locally-computed basis functions, associated to the mechanical and flow problems (Sokolova et al. 2019). These basis functions are computed at the beginning of the simulation by solving the local problems at each coarse grid cell. Details of this procedure for mechanical deformation under nonlinear creep can be found in Ramesh Kumar and Hajibeygi (2021). In this work, flow and mechanics basis functions are solved independently; and used to construct the block diagonal prolongation and restriction operators.

## 5 Results

In this section, numerical results of the above formulation are presented. The well-known Mandel test case is studied for benchmarking linear finescale and multiscale elastic poromechanics. The schematic is shown in Fig. 2. The problem describes an infinitely long poroelastic slab bounded by impermeable plates with fluid. A load is applied on the top face at  $t = 0$ , and the drainage is allowed from the east boundary.

Figure 3 shows the poroelastic Mandel test case simulation results for both finescale and multiscale. The parameters chosen for this test case are shown in Table 1. The analytical formulation is obtained from (Wang 2000).

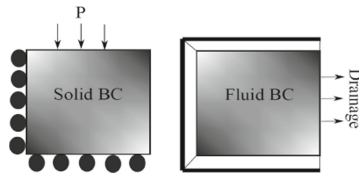


**Fig. 2.** The above illustration shows the schematic of Mandel test case. The domain is subjected to roller constraint at south, west, a traction free surface in the east and a constant load is applied on the top face. Drainage is allowed in the east face.

Figure 3a shows the variation of the pressure along the horizontal distance along the domain. The overpressure at the initial timesteps is caused due to the contraction at

**Table 1.** The parameters chosen for Mandel test case for poroelastic and poro-inelastic domain.

Load	2 Pa	Time step	0.009 s	$t_{end}$	0.89 s
Grid	$24 \times 2 \times 24$	Poisson ratio	0.2	M	1e100 Pa
Q	60000 J/mole	E	1e4 Pa	b	1
A	5e4	n	2.5	T	300 K

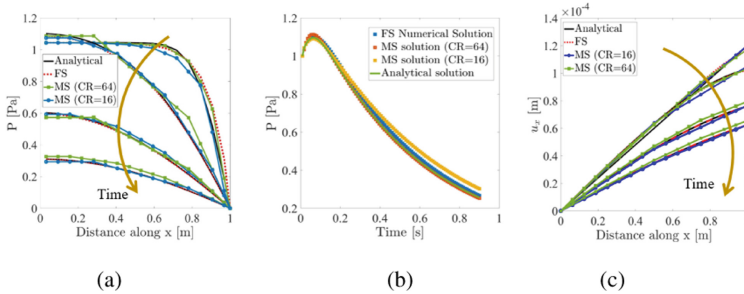


**Fig. 3.** The above illustrations show the a) variation of pressure along the domain in horizontal direction, b) variation of pressure with time and c) variation of horizontal deformation along the domain in horizontal direction at four time instants  $[0.01, 0.1, 0.5, 0.9] \times t_{end}$ , for the grid size of  $24 \times 2 \times 24$  for both finescale and multiscale poroelastic domain. Note that for multiscale (MS) simulations the coarsening ratios (CR) of 16 (i.e.,  $4 \times 4$ ) and 64 (i.e.,  $8 \times 8$ ) are used.

the plate’s drained edges, causing a buildup in the pore pressure. It can be seen that the multiscale solution for coarsening ratio of 64 is not accurate compared to the finescale solution. This could be further improved by using an iterative MS strategy beyond the scope of this work Ramesh Kumar and Hajibeygi (2021). Figure 3b shows the pressure variation with time for finescale and multiscale grids of different coarsening. It can be seen that the trend is captured well by the MS procedure; however, the jump in the pressure initially is slightly different from the analytical and finescale solution. Figure 3c shows the variation of the horizontal displacement with distance along the domain of the homogeneous rock. It can be seen that the MS pressure and deformation are very close to the finescale and analytical solutions for homogeneous poroelastic rocks.

This test case is further analyzed when the rocks are considered inelastic and undergo creep deformation. The parameters chosen for the creep formulation are presented in Table 1. The chosen parameters are adopted in order to study the effect of creep deformation on the poro-mechanical system both at finescale and multiscale. Figure 4 shows the results of the simulation. Figure 4a and b show the results of pressure and horizontal displacement along the x-axis when creep is incorporated. The effect of creep is not prominently seen in these graphs, which are very similar to Fig. 3a and Fig. 3c. To further quantify the effect of creep, the difference of the solutions with the elastic domain is presented in Fig. 4c and 4d for both displacement and pressure, respectively. They are shown along the horizontal distance for time instants  $[0.01, 0.05, 0.10, 0.15, 0.5, 0.9] \times t_{end}$ . It can be seen that the difference in displacement and pressure increases



with time which is caused due to permanent inelasticity that is incorporated. Secondly, for time instants  $t_2$  and  $t_3$  the change in displacement and pressure is not smooth. This could be caused by a sudden buildup of pore pressure in the initial timesteps, resulting in non-uniform stress distribution in the domain. The magnitude of increase in pressure and deformation caused due to creep is around 1%.

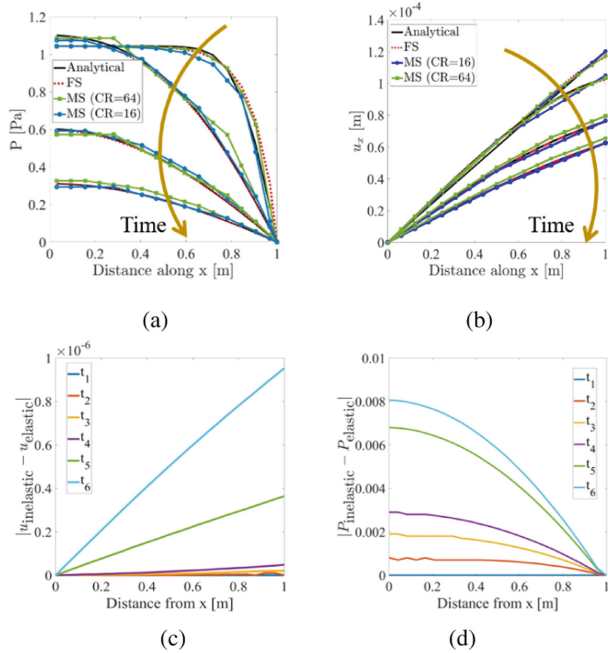


**Fig. 4.** The above illustrations show the (a) variation of pressure with time, (b) variation of pressure along the domain in horizontal direction for time instants time instants  $[0.01, 0.1, 0.5, 0.9] \times t_{end}$  and (c) show the difference between the inelastic and elastic deformation and (d) show the difference between the inelastic pressure and elastic pressure at time instants  $[0.01, 0.05, 0.10, 0.15, 0.5, 0.9] \times t_{end}$ .

The effect of creep using synthetic input parameters was not so pronounced in this test case. However, with high heterogeneity in the physical domain and the parameters chosen from the experimental data the effects of creep could be significant.

## 6 Conclusions

Successful scaling up of this technology requires, among others, scalable simulation methods for nonlinear poromechanical systems. In this work, after developing a fully-implicit fine-scale hybrid FE-FV scheme, an algebraic multiscale strategy, consistent with the hybrid FE-FV fine-scale formulation, was developed. This allows for field relevant test cases, in which heterogeneous geo-models are required to be solved for many possible realizations. As a proof-of-the-concept, the well-studied Mandel test

case was investigated in more details, especially on the applicability of the multiscale method for coupled systems in the presence of creep.

Future work involves studying heterogeneous systems, with viscoplasticity and thermos-plasticity included. Sensitivity analysis and uncertainty quantification will be also studied in future developments, for specific potential sites. The developed multiscale strategy does not rely on any upscaling of parameters, aims at mapping the solution space between fine and coarse scale; and thus can be employed for accurate and efficient field relevant studies.

**Acknowledgements.** The financial support of NWO-TTW ViDi grant (project ADMIRE 17509) is acknowledged. The authors would like to thank all members of ADMIRE.

## References

- Hashemi, L., Blunt, M., Hajibeygi, H.: Pore-scale modelling and sensitivity analyses of hydrogen-brine multiphase flow in geological porous media. *Sci. Rep.* **11**(1), 1–13 (2021)
- Tarkowski, R.: Underground hydrogen storage: characteristics and prospects. *Renew. Sustain. Energy Rev.* **105**, 86–94 (2019)
- Zivar, D., Kumar, S., Foroozesh, J.: Underground hydrogen storage: a comprehensive review. *Int. J. Hydrogen Energy* **46**(45), 23436–23462 (2021)
- Ramesh Kumar, K., Hajibeygi, H.: Multiscale simulation of inelastic creep deformation for geological rocks. *J. Comput. Phys.* **440**, 110439 (2021)
- Firme, P., Roehl, D., Romanel, C.: Salt caverns history and geomechanics towards future natural gas strategic storage in brazil. *J. Nat. Gas Sci. Eng.* **72**, 103006 (2019)
- Ramesh Kumar, K., Makhmutov, A., Spiers, C.J., Hajibeygi, H.: Geomechanical simulation of energy storage in salt formations. *Sci. Rep.* **11**, 19640 (2021)
- Carter, N., Horseman, S., Russell, J., Handin, J.: Rheology of rocksalt. *J. Struct. Geol.* **15**, 1257–1271 (1993)
- Biot, M.A.: General theory of three-dimensional consolidation. *J. Appl. Phys.* **12**, 155–164 (1941)
- Castelletto, N., White, J.A., Tchelepi, H.A.: Accuracy and convergence properties of the fixed-stress iterative solution of two-way coupled poromechanics. *Int. J. Numer. Anal. Meth. Geomech.* **39**(14), 1593–1618 (2015)
- Castelletto, N., Hajibeygi, H., Tchelepi, H.A.: Multiscale finite-element method for linear elastic geomechanics. *J. Comput. Phys.* **331**, 337–356 (2017)
- Sokolova, I., Bastisya, M.G., Hajibeygi, H.: Multiscale finite volume method for finite-volume-based simulation of poroelasticity. *J. Comput. Phys.* **379**, 309–324 (2019)
- Wang, H.: *Theory of Linear Poroelasticity*. Princeton University Press, Princeton (2000)